ISSN 0208-7774 TRIBOLOGIA 3/2021 p. 19–26
DOI: 10.5604/01.3001.0015.6893

Michał KEKEZ[*], Wojciech JURCZAK[**], Dariusz OZIMINA[***]

CLASSIFICATION AND MODELLING OF SOUND EMISSION SIGNALS IN SELECTED TRIBOSYSTEMS

KLASYFIKACJA I MODELOWANIE SYGNAŁÓW DŹWIĘKU W WYBRANYCH SYSTEMACH TRIBOLOGICZNYCH

Key words: tribosystem, sound level, regression trees, random forest.

Abstract: The paper presents an analysis of the sound level recorded during dry sliding friction conditions. Balls with a diameter of 6 mm placed on pins were made of 100Cr6 steel, silicon carbide (SiC), and corundum (Al_2O_3), while rotating discs with a height of 6 mm and a diameter of 42 mm were made of 100Cr6 steel. Each pin and disc system was tested for two values of the relative humidity of the air (50 ± 5% and 90 ± 5%). Models of the A-sound level were developed using regression trees and random forest. The paper presents an analysis of the accuracy of the models obtained. Classifications of the six tests performed on the basis of sound level descriptors were also carried out.

Słowa kluczowe: system tribologiczny, poziom dźwięku, drzewa regresji, las losowy.

Streszczenie: W pracy przedstawiono analizę poziomu dźwięku zarejestrowanego podczas tarcia technicznie suchego w ruchu ślizgowym. Podczas sześciu testów tribologicznych stosowano próbkę wykonaną ze stali 100Cr6 oraz trzy przeciwpróbki, wykonane ze stali 100Cr6, węglika krzemu (SiC) i korundu (Al_2O_3), przy czym każdy układ próbka – przeciwpróbka był testowany dla dwóch wartości wilgotności względnej powietrza (50 ± 5% i 90 ± 5%). Opracowano modele poziomu dźwięku A z użyciem drzew regresji i lasu losowego. W pracy zamieszczono analizę dokładności otrzymanych modeli. Została również przeprowadzona klasyfikacja sześciu wykonanych testów w oparciu o deskryptory poziomu dźwięku.

INTRODUCTION

In tribosystems, the resistance attributable to friction is overcome by applying energy that can be dissipated, accumulated, or transformed **[L. 1]**. The phenomena that occur during friction are, among others, acoustic emission (AE) and the emission of sound **[L. 2]**.

Stick-slip friction can be analysed using acoustic emission **[L. 3]**. AE was also used to detect the transition between mild and severe wear in metal sliding **[L. 4]**. The acoustic emission generated from the sliding contact of metal-metal pairs using pin-on-disk tests was investigated in **[L. 5]**. Computational intelligence methods, including genetic algorithms and artificial neural networks, were used in **[L. 6]** to classify acoustic emission signals from journal bearings. Certain frequencies in AE reflect friction, while others reflect wear during ball-on-disc reciprocating tribological tests **[L. 7]**. The features of the AE signals generated during adhesive wear and abrasive mechanical wear were examined in **[L. 8]**. Experiments carried out on a pin-on-disc tribometer with a sliding silicon nitride or M50 ball on a silicon nitride or M50NiL steel flat disc

[*] ORCID: 0000-0001-9521-0788. Kielce University of Technology, Faculty of Mechatronics and Mechanical Engineering, Tysiąclecia Państwa Polskiego 7 Ave., 25-314 Kielce, Poland.
[**] ORCID: 0000-0002-1608-7249. Polish Naval Academy, Faculty of Mechanical and Electrical Engineering, Jana Śmidowicza 69 Street, 81-127 Gdynia, Poland.
[***] ORCID: 0000-0001-5099-6342. Kielce University of Technology, Faculty of Mechatronics and Mechanical Engineering,Tysiąclecia Państwa Polskiego 7 Ave., 25-314 Kielce, Poland.

showed that the RMS of the acoustic emission signal has a good correlation with friction **[L. 9]**. Acoustic emission signals with a peak frequency of around 1 MHz occur during adhesive wear and with a peak frequency of around 0.5 MHz during abrasive wear, which can be detected in real time **[L. 10]**.

Noise and vibration induced by stick-slip friction in an instrument panel were investigated in **[L. 11]**. Vibration and noise in a gear mesh and a method of its attenuation were presented in **[L. 12]**. Numerical simulations of friction noise of two rough and dry surfaces were studied in **[L. 13]**. Vibration and noise when a sphere is sliding on a groove-textured surface were discussed (with sound frequency analysis) in **[L. 14]**.

METHODOLOGY AND MATERIALS

Tribological tests (**Table 1**) were performed on the TRB3 ball-on-disc tribometer (**Fig. 1**). Balls with a diameter of 6 mm were made of 100Cr6 steel, silicon carbide (SiC), and corundum (Al_2O_3), while rotating discs with a height of 6 mm and a diameter of 42 mm were made of 100Cr6 steel. All tests were conducted under technically dry friction conditions. The sliding distance was 1000 m.

Table 1. Parameters of tribological tests [L. 15]
Tabela 1. Parametry testów tribologicznych **[L. 15]**

Parameter	Unit	Value
Load	N	15
Sliding rate	m/s	0.07
Sliding distance	m	1000
Temperature	°C	25±1

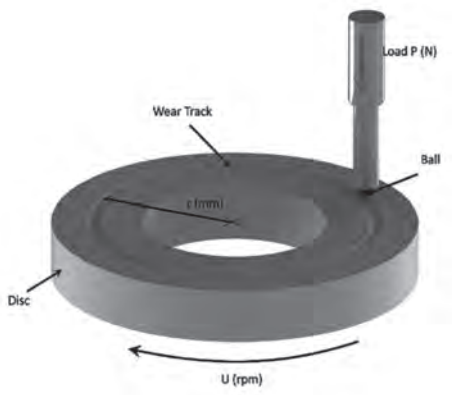

Fig. 1. Ball-on-disc diagram (b) [L. 16]
Rys. 1. Schemat węzła tarcia typu ball-on-disc (b) [L. 16]

The ball and disc materials, as well as the relative humidity of the air, are shown in **Table 2**. Tests 1 and 4 were carried out for the discs and balls made of 100Cr6 steel. Tests 2 and 5 were carried out for the discs made of 100Cr6 steel and the balls made of Al_2O_3, and Tests 3 and 6 were carried out for the discs made of 100Cr6 steel and the balls made of SiC.

Table 2. Materials used and conditions for tribological tests
Tabela 2. Zastosowane materiały i warunki testów tribologicznych

Disc	Ball	Air relative humidity 50 ± 5%	Air relative humidity 90 ± 5%
100Cr6 steel	100Cr6 steel	Test 1	Test 4
100Cr6 steel	Al_2O_3	Test 2	Test 5
100Cr6 steel	SiC	Test 3	Test 6

During the tests, A-, C- and Z-weighted sound levels (as well as 1/3-octave band sound levels) were recorded every 100 milliseconds using a Svantek SVAN971, which is a Class 1 sound level meter and analyser with 24-bit analogue-to-digital converter **[L. 17]** and antialiasing filter. Next, the A-weighted equivalent sound levels L_{Aeq} were calculated for each 10-second period of time using equation (1) **[L. 18]**:

$$L_{Aeq} = 10\log\left(\frac{1}{N}\sum_{i=1}^{N}10^{0.1L_{A,i}}\right), \qquad (1)$$

where $N = 100$ and $L_{A,i}$ values (A-weighted) come from 100 consecutive 100-milisecond sound levels. During the tests, the sound was recorded using an Olympus LS-P1 Linear PCM Recorder in such a way that the analogue audio signal was sampled with 44100 Hz frequency and stored in 16-bit digital linear PCM (pulse-code modulation) format.

RESULTS AND DISCUSSION

Figures 2 and **3** present 10-second L_{Aeq} values as a function of time in tribological Tests 1 to 6. For tests conducted in 50% relative humidity (**Fig. 2**), the greatest variability of the sound level occurred in Test 1 (with the sound level gradually increasing

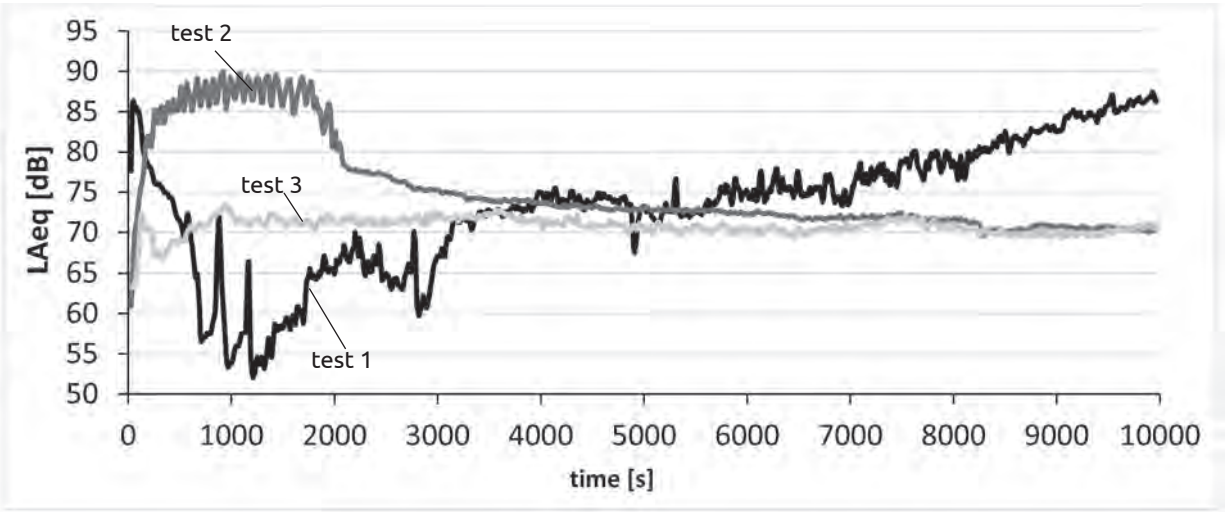

Fig. 2. Equivalent sound level L_{Aeq} in 10-second time intervals, for tests conducted when relative humidity equals 50 ± 5%: test 1, test 2, test 3

Rys. 2. Równoważny poziom dźwięku L_{Aeq} w 10-sekundowych odcinkach czasu dla testów tribologicznych przeprowadzonych przy wilgotności względnej 50 ± 5%: test 1, test 2, test 3

in the last 5000 seconds) and the smallest variability occurred in Test 3.

The relative humidity of the air of 90% (**Fig. 3**) resulted in lower sound levels in the first 800 seconds of Tests 4, 5, and 6, and in increased sound level variability in Tests 4 and 5 in the last 5000 seconds, compared to similar tests (1, 2, and 3, respectively) made at the humidity of 50%.

Figures 4 and **5** show how relative humidity affected the minimum, maximum, and variance of L_{Aeq} values.

Equivalent sound levels for the Tests 1 to 6 are shown in **Table 3**. The highest values (above 80 dB) were recorded for Tests 4 and 2, while the lowest values (below 71 dB) were observed for Tests 3 and 6.

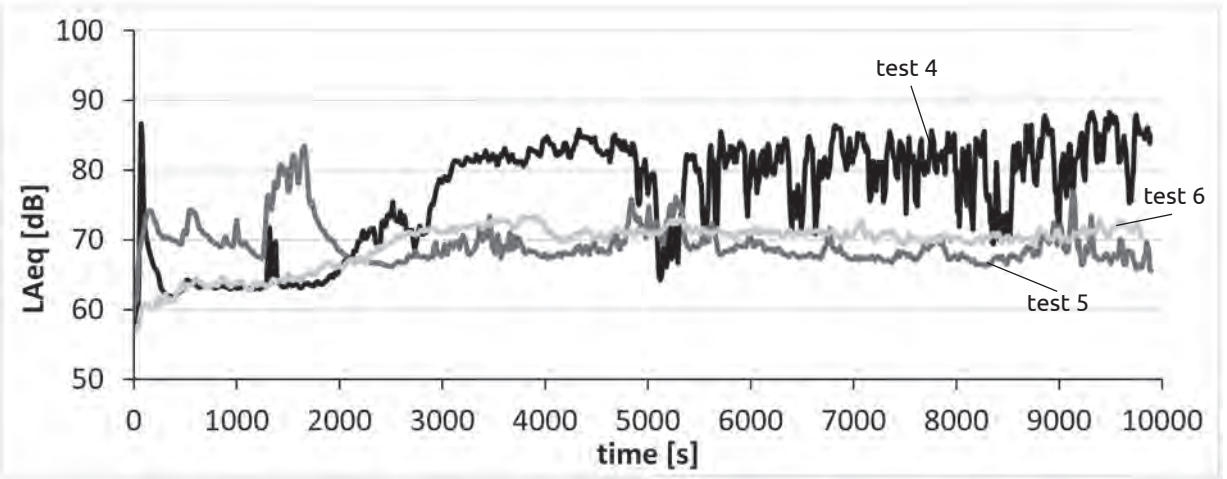

Fig. 3. Equivalent sound level L_{Aeq} in 10-second time intervals, for tests conducted when relative humidity equals 90 ± 5%: test 4, test 5, test 6

Rys. 3. Równoważny poziom dźwięku L_{Aeq} w 10-sekundowych odcinkach czasu, dla testów tribologicznych przeprowadzonych przy wilgotności względnej 90 ± 5%: test 4, test 5, test 6

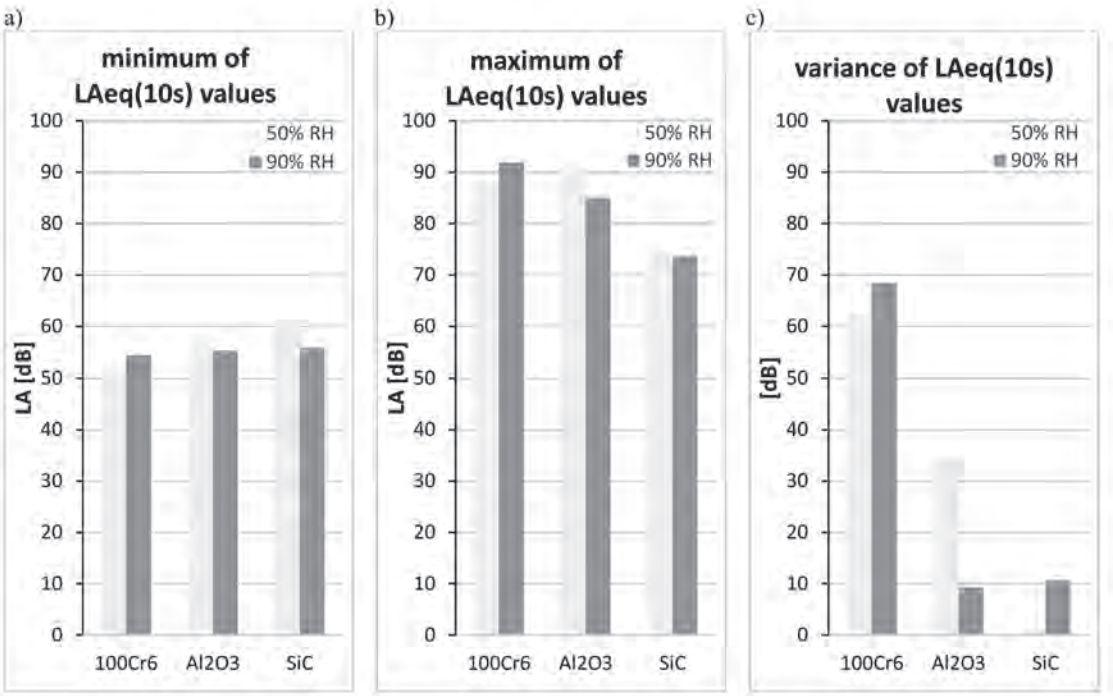

Fig. 4. Minimum (a), maximum (b), and variance (c) of the values of equivalent sound level L_{Aeq} in 10-second time intervals, for tests conducted when relative humidity equals 50 ± 5% (tests 1, 2, and 3) or 90 ± 5% (tests 4, 5, and 6)

Rys. 4. Minimum (a), maksimum (b) i wariancja (c) wartości równoważnego poziomu dźwięku L_{Aeq} w 10-sekundowych odcinkach czasu dla testów tribologicznych przeprowadzonych przy wilgotności względnej 50 ± 5% (testy 1, 2, 3) lub 90 ± 5% (testy 4, 5, 6)

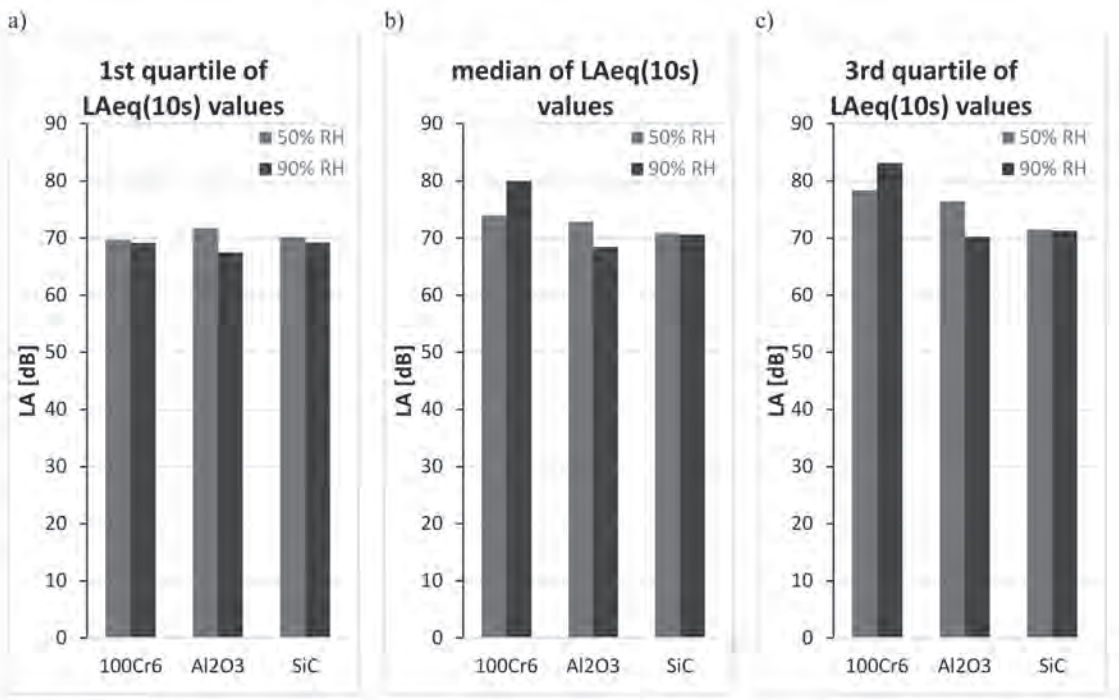

Fig. 5. The first quartile (a), the median (b), and the third quartile (c) of values of equivalent sound level L_{Aeq} in 10-second time intervals, for tests conducted when relative humidity equals 50 ± 5% (tests 1, 2 and 3) or 90 ± 5% (tests 4, 5 and 6)

Rys. 5. Pierwszy kwartyl (a), mediana (b) i trzeci kwartyl (c) wartości równoważnego poziomu dźwięku L_{Aeq} w 10-sekundowych odcinkach czasu dla testów tribologicznych przeprowadzonych przy wilgotności względnej 50 ± 5% (testy 1, 2, 3) lub 90 ± 5% (testy 4, 5, 6)

Table 3. Equivalent sound levels for the whole tribological test

Tabela 3. Równoważny poziom dźwięku z całego testu tribologicznego

Test	L_{Aeq} for the whole test
1	78.5 dB
2	80.6 dB
3	70.9 dB
4	81.4 dB
5	71.2 dB
6	70.2 dB

MODELS OF SOUND LEVEL VARIABILITY

The L_{Aeq} values for 10-second intervals together with time values formed 6 training datasets (one for each of the 6 tribological tests). The only input attribute was time, and the output attribute was L_{Aeq}. Then, the random forest algorithm **[L. 19]** implemented in a Weka software package **[L. 20]** was used separately for each of the training datasets and produced 6 models of sound variability. The random forest of regression trees **[L. 19]** belongs to the group of computational intelligence methods that are widely used to build models or analyse data. The accuracies of the six models created by

Table 4. RMSE errors of the models estimated by 10-fold cross validation

Tabela 4. Błędy RMSE modeli oszacowane za pomocą 10-krotnej walidacji krzyżowej

Test number and model number	RMSE [dB]
1	1.5980
2	0.7488
3	0.4486
4	3.8384
5	1.2796
6	0.4482

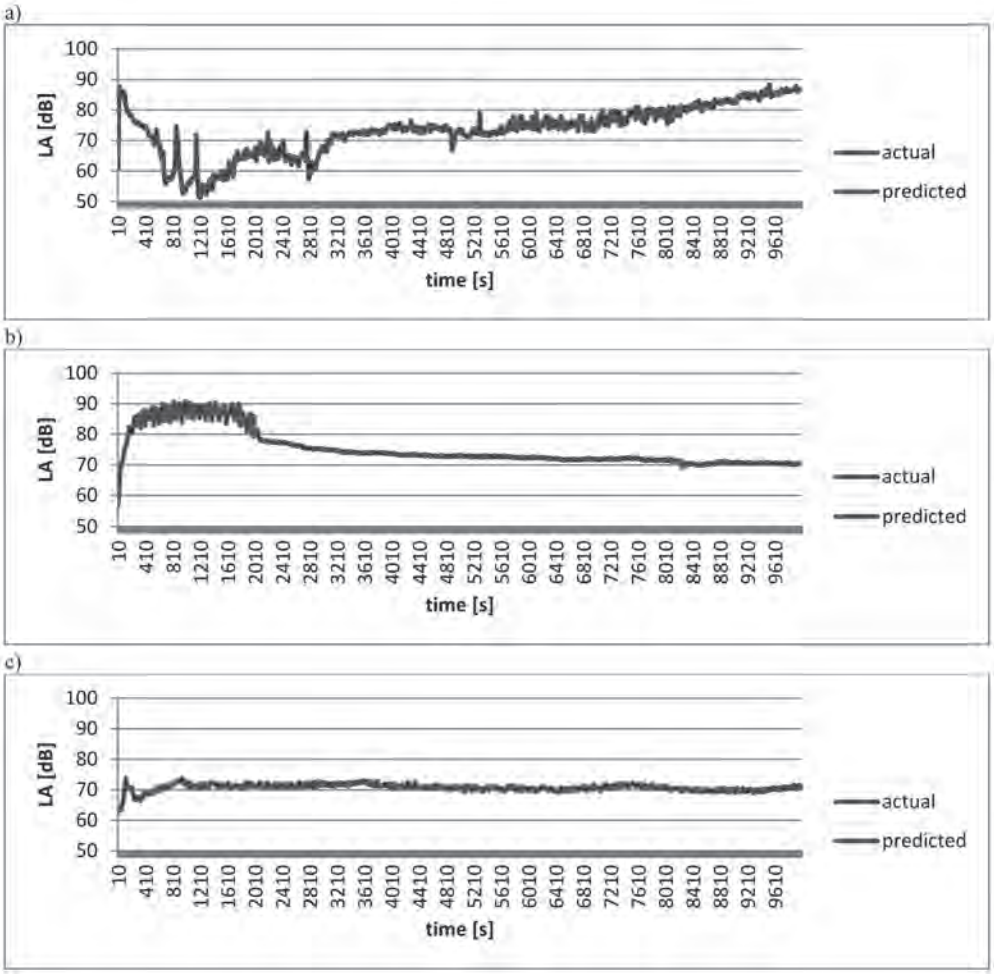

Fig. 6. The 10-second L_{Aeq} values (actual and predicted by the model) for tribological tests at 50% relative air humidity: a) test 1, b) test 2, c) test 3

Rys. 6. Wartości 10-sekundowego L_{Aeq} (obliczone z wartości zarejestrowanych podczas testu tribologicznego oraz obliczone przez model) przy 50% wilgotności względnej powietrza: a) test 1, b) test 2, c) test 3

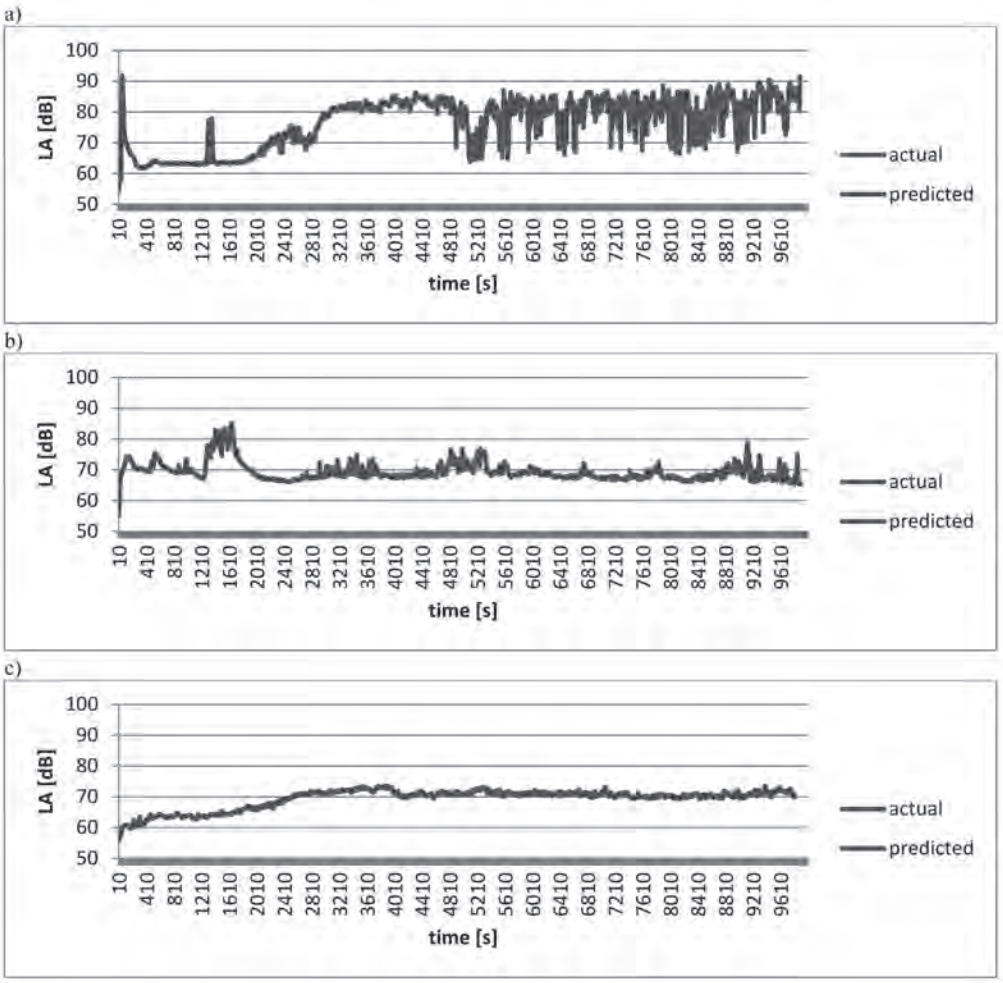

Fig. 7. The 10-second L_{Aeq} values (actual and predicted by the model) for tribological tests at 90% relative air humidity: a) test 4, b) test 5, c) test 6

Rys. 7. Wartości 10-sekundowego L_{Aeq} (obliczone z wartości zarejestrowanych podczas testu tribologicznego oraz obliczone przez model) przy 90% wilgotności względnej powietrza: a) test 4, b) test 5, c) test 6

random forest were estimated using the 10-fold cross validation method, and the resulting RMSE (root mean square errors) are shown in **Table 4**. The most accurate models were obtained for the 100Cr6-SiC pair (Tests 3 and 6), and quite good models were obtained for the 100Cr6-Al_2O_3 pair (Tests 2 and 5). **Figures 6** and **7** show the 10-second L_{Aeq} values (experimental and modelled) for tribological tests performed at 50% relative air humidity (**Fig. 6**) and at 90% relative air humidity (**Fig. 7**).

CLASSIFICATION OF TESTS BASED ON SOUND LEVEL

Five descriptors characterizing the course of the equivalent sound level in 10-second intervals (L_{Aeq}) were developed: a_1 and a_2 – respectively, minimum and maximum of L_{Aeq} values in the range from 500 to 2000 seconds from the start of the test; a_3 and a_4 – respectively, minimum and maximum of L_{Aeq} values in the range from 5000 to 10,000 seconds from the start of the test; and, a_5 – the variance of L_{Aeq} values in the time range from 5000 to 10,000 seconds from the start of the test (attribute). The values of these descriptors are presented in **Table 5**.

Based on the data in **Table 5**, the following classifier was created:

– if a_5>27.5 then the test number is 4 (100Cr6 steel on 100Cr6 steel, about 90% RH)
– if 12.3<a_5< = 27.5 then the test number is 1 (100Cr6 steel on 100Cr6 steel, about 50% RH)
– if a_5< = 12.3 and a_1>74.0 then the test number is 2 (Al_2O_3 on 100Cr6 steel, about 50% RH)

Table 5. Developed descriptors of the course of 10-second L_{Aeq}
Tabela 5. Opracowane deskryptory przebiegu 10-sekundowego L_{Aeq}

a_1 [dB]	a_2 [dB]	a_3 [dB]	a_4 [dB]	a_5 [dB]	Test
51.2	74.7	71.1	88.3	20.1	1
79.3	90.9	69.0	73.3	0.8	2
68.8	73.8	68.9	72.3	0.4	3
62.7	77.8	63.8	91.5	35.0	4
67.1	85.0	65.3	78.8	4.5	5
62.7	67.0	69.2	73.5	0.7	6

- if $a_5 <= 12.3$ and $a_1 <= 74.0$ and $a_2 > 81.4$ then the test number is 5 (Al_2O_3 on 100Cr6 steel, about 90% RH)
- if $a_5 <= 12.3$ and $a_1 <= 74.0$ and $70.4 < a_2 <= 81.4$ then the test number is 3 (SiC on 100Cr6 steel, about 50% RH)
- if $a_5 <= 12.3$ and $a_1 <= 74.0$ and $a_2 <= 70.4$ then the test number is 6 (SiC on 100Cr6 steel, about 90% RH)
- where RH means the relative humidity of the air.

This classifier allows us to determine the material pair used in the test and whether the relative humidity was about 50% or about 90%.

CONCLUSIONS

Based on the measurements and calculations performed, the following conclusions were formulated:

a) The lowest variability of the sound level was observed for the 100Cr6 – SiC pair.
b) The greatest variability of the sound level was observed for the 100Cr6 – 100Cr6 pair.
c) The most accurate models of sound level variability were created for the 100Cr6 – SiC pair (RMSE<0.45 dB).
d) The sound level variability models for the 100Cr6 – Al_2O_3 pair have quite good accuracy (RMSE<1.28 dB).
e) The sound level variability models for the 100Cr6 – 100Cr6 pair are the least accurate due to the very large and random variability of the sound level over time.

REFERENCES

1. Kajdas Cz., Kulczycki A., Ozimina D.: A new concept of the mechanism of tribocatalytic reactions induced by mechanical forces, "Tribology International" 2017, 107, pp. 144–151.
2. Kekez M., Desaniuk T., Duszczyk J., Ozimina D.: On the use of acoustic emission to assess the wear in a tribosystem, "Journal of Machine Construction and Maintenance" 2019, 2, pp. 99–103.
3. Ferrer C., Salas F., Pascual M., Orozco J.: Discrete acoustic emission waves during stick-slip friction between steel samples, "Tribology International" 2010, 43, pp. 1–6.
4. Hanchi J., Klamecki B.E.: Acoustic emission of the wear process, "Wear" 1991, 145, pp. 1–27.
5. Jiaa C.L., Dornfeld D.A.: Experimental studies of sliding friction and wear via acoustic emission signal analysis, "Wear" 1990, 139, pp. 403–424.
6. Sadegh H., Mehdi A.N., Mehdi A.: Classification of acoustic emission signals generated from journal bearing at different lubrication conditions based on wavelet analysis in combination with artificial neural network and genetic algorithm, "Tribology International" 2016, 95, pp. 426–434.
7. Geng Z., Puhan D., Reddyhoff T.: Using acoustic emission to characterize friction and wear in dry sliding steel contacts, "Tribology International" 2019, 134, pp. 394–407.
8. Hase A., Mishina H., Wada M.: Correlation between features of acoustic emission signals and mechanical wear mechanisms, "Wear" 2012, 292–293, pp. 144–150.

9. Wang L., Wood R.J.K.: Acoustic emissions from lubricated hybrid contacts, "Tribology International" 2009, 42, pp. 1629–1637.
10. Hase A., Wada M., Mishina H.: Scanning electron microscope observation study for identification of wear mechanism using acoustic emission technique, "Tribology International" 2014, 72, pp. 51–57.
11. Rorrer R.A.L., Juneja V.: Friction-induced vibration and noise generation of instrument panel material pairs, "Tribology International" 2002, 35, pp. 523–531.
12. Ene N.M., Dimofte F.: Effect of fluid film wave bearings on attenuation of gear mesh noise and vibration, "Tribology International" 2012, 53, pp. 108–114.
13. Ben Abdelounis H, Zahouani H., Le Bot A., Perret-Liaudet J., Ben Tkaya M.: Numerical simulation of friction noise, "Wear" 2011, 271, pp. 621–624.
14. Wang D.W., Mo J.L., Wang Z.G., Chen G.X., Ouyang H., Zhou Z.R., Numerical study of friction-induced vibration and noise on groove-textured surface, "Tribology International" 2013, 64, pp. 1–7.
15. Desaniuk T., Soboń D., Jurczak W.: Effect of humidity on tribological properties of selected friction junctions with evaluation of acoustic emission, "Tribologia" 2021, accepted.
16. Ozimina D., Madej M., Desaniuk T., Żółty M., Kulczycki A.: Effects of a graphene-enhanced lubricant on the performance of a tribosystem, "Journal of Machine Construction and Maintenance" 2019, 2, pp. 75–81.
17. Szcześniak A., Myczuda Z.: A method of charge accumulation in the logarithmic analog-to-digital converter with a successive approximation, "Przegląd Elektrotechniczny" 2010, 10, pp. 336–340.
18. International Organization for Standardization: Acoustics – Determination of occupational noise exposure – Engineering method. ISO 9612:2009.
19. Breiman L.: Random Forests, "Machine Learning" 2001, 45(1), pp. 5–32.
20. Frank E., Hall M.A., Witten I.H.: The WEKA Workbench. Online Appendix for "Data Mining: Practical Machine Learning Tools and Techniques", Morgan Kaufmann, Fourth Edition, 2016.